$$|I_{qq'}|^2 = \tfrac{1}{4}[C^2 + D^2 - \tfrac{1}{8}k^2(C^2 - D^2)(1 + k_{33}/k_{11})] \times (\delta_{q',q+\pi/Z} + \delta_{q',q-\pi/Z}) \quad . \tag{4.36}$$

As in Sec. III we suppose that unpolarized light is incident at an angle θ to the z axis and is scattered by an angle γ. As before, the scattering is assumed to take place in a plane including the z axis which makes an angle ϕ with the direction of the magnetic field (see Fig. 2). Averaging over both polarization directions of the incident and scattered light gives

$$A^2 = \tfrac{1}{4}[(1 + t_1^2c^2)(1 + t_2^2s^2)]^{-1} + \tfrac{1}{4}[(1 + t_2^2c^2)(1 + t_1^2s^2)]^{-1} \ ,$$

$$B^2 = \tfrac{1}{4}[(1 + t_1^2s^2)(1 + t_2^2s^2)]^{-1} + \tfrac{1}{4}[(1 + t_1^2c^2)(1 + t_2^2c^2)]^{-1} \ ,$$

$$C^2 = \frac{1}{4}\left(\frac{s_2^2}{1 + t_1^2s^2} + \frac{s_1^2}{1 + t_2^2s^2} + \frac{2s_1s_2s^2}{[(1 + t_1^2s^2)(1 + t_2^2s^2)]^{1/2}}\right) \ ,$$

and D^2 is obtained from C^2 by replacing s by c. In these formulas we have

$$t_1 = \tan\theta, \quad t_2 = \tan(\theta + \gamma), \quad s_1 = \sin\theta, \quad s_2 = \sin(\theta + \gamma), \quad s = \sin\phi, \quad c = \cos\phi \ .$$

Summarizing we might say that a magnetic field applied perpendicularly to the cholesteric axis leads to the following changes in the light scattering properties:

(i) The peaks in the intensity are displaced owing to the change in pitch.

(ii) Even with the Born approximation, peaks appear at the higher-order Bragg angles (we expect this to be true also for the viscous-splay mode to higher order in the field). This effect is due to the higher harmonics of the helical structure.

(iii) The q dependence of the linewidth is altered in a very sensitive way and in fact now exhibits a gaplike structure. Note that the pitch for the two curves in Fig. 1 has changed by only about 1%.

(iv) The angular dependence of the scattered intensities becomes more complex.

Measurements of the predicted effects should lead to valuable information about the elastic constants and viscosities of cholesteric liquid crystals.

*Supported in part by the National Science Foundation.

[1]See e.g., I. G. Chistyakov, Usp. Fiz. Nauk 89, 563 (1966) [Soviet Phys. Usp. 9, 551 (1966)].

[2]Groupe d'Etude des Cristaux Liquides (Orsay), J. Chem. Phys. 51, 816 (1969).

[3]P. G. de Gennes, Solid State Commun. 6, 163 (1968).

[4]C. W. Oseen, Trans. Faraday Soc. 29, 883 (1933).

[5]F. C. Frank, Discussions Faraday Soc. 25, 19 (1958).

[6]J. L. Ericksen, Arch. Ratl. Mech. Anal. 4, 231 (1960).

[7]F. M. Leslie, Quart. J. Mech. Appl. Math. 19, 357 (1966).

[8]M. J. Stephen, Phys. Rev. (to be published).

[9]O. Parodi, J. Phys. (to be published).

[10]This was pointed out to us by P. Hohenberg.

[11]E. T. Whittaker and G. N. Watson, *Modern Analysis* (Cambridge U. P., Cambridge, England, 1940).

[12]P. Lebwhol and M. J. Stephen, Phys. Rev. 163, 376 (1967).

PHYSICAL REVIEW A VOLUME 2, NUMBER 6 DECEMBER 1970

Attenuation Coefficients of Gases for 4.5–145-keV Photons*

J. H. McCrary, L. D. Looney, and C. P. Constanten†
EG & G, Incorporated, Las Vegas, Nevada 89101

and

H. F. Atwater
University of California, Los Alamos Scientific Laboratory, Los Alamos, New Mexico 87544

(Received 22 May 1970)

Narrow-beam mass-attenuation coefficients were measured for air, neon, argon, krypton, and xenon. Radioisotope sources were used to provide photons whose energies were 4.508, 5.895, 9.243, 27.380, 44.229, 88.09, and 145.43 keV. Experimental errors were less than 2% for all measurements. The experimental results are compared with theoretical predictions of the attenuation coefficients.

I. INTRODUCTION

In the energy region of 1–20 keV, extensive measurements have been made of the attenuation coefficients of neon and argon.[1–9] Above 20 keV, very few experimental results are available.[8,9] For photon energies greater than 3 keV, relatively few attenuation coefficients have been measured for air,[5–7,10] krypton,[9,11,12] and xenon.[12] Rau and Fano[13] suggest that irregularities in photon cross sections

are likely to occur with the interpolation of these cross sections with respect to Z for the noble gases. In an attempt to improve the present knowledge of gas photon cross sections, an experiment was designed wherein the narrow-beam mass-attenuation coefficients of air, neon, argon, krypton, and xenon would be measured with an accuracy of $\pm 1-2\%$ at seven energies between 4.5 and 145 keV.

The narrow-beam mass-attenuation coefficient μ/ρ, with units of cm^2/g, is defined by the relation

$$I/I_0 = e^{-(\mu/\rho)x}, \quad (1)$$

where I/I_0 is the gas transmissivity and x is the sample thickness in g/cm^2.

II. APPARATUS

The experimental arrangement is shown schematically in Fig. 1. Since the measured mass-attenuation coefficients ranged through four orders of magnitude, many different sample lengths and sample densities were required. Sample lengths 10–733 cm and sample pressures 30–3600 Torr were used. The solid angle subtended by the detector at the source varied between 7×10^{-3} and 1.5×10^{-5} sr.

The gas chamber shown in Fig. 1 was made from sections of brass pipe which were $5\frac{1}{4}$-in. i.d. $\times 5\frac{1}{2}$-in. o.d. Several 1-, 2-, and 4-ft lengths of this pipe were equipped with O-ringed end flanges which could be bolted together to provide the needed gas sample length. The pipes were cleaned and leak checked prior to use.

From one to three collimators were spaced at equal intervals between the source and the detector to minimize scattering from the walls of the pipe and from the gas. The collimators were made from Pb sufficiently thick to stop virtually all of the source radiation. The collimator apertures were in every case slightly larger than the cone subtended by the detector at the source. The number of collimators was determined by the sample length. Longer sample lengths were used with the higher-energy photon sources. Thus in the energy region where scattering is more important, more collimation was used.

One of the 2-ft sections of pipe was equipped with gas-handling and gas-sampling apparatus. Experiments involving sample lengths of less than 2 ft were performed by placing the source, detector, and collimator on a track inside the gas-handling section of pipe. A large mechanical pump was used to evacuate the chamber. The vacuum condition was read on a thermocouple vacuum gauge. All vacuum counts were taken at pressures of less than 5×10^{-3} Torr.

Gas pressures of less than 1 atm were measured with a closed-end Hg manometer and cathetometer. The accuracy of these measurements was ± 0.3 Torr. Pressures greater than 1 atm were measured with a Heise Bourdon tube pressure gauge whose accuracy was ± 5 Torr. Room-air (and thus sample) temperature was measured with a Hg thermometer which was checked against two Weather Bureau secondary standard thermometers. The accuracy of the temperature measurements was $\pm 0.2\,^{\circ}C$. Sample temperatures ranged from 21 to 27 °C. Measurements of sample lengths greater than 60 cm were made with a steel tape whose accuracy was checked with a precision cathetometer. The accuracy of these measurements was ± 0.5 mm. The shorter lengths were set with metal measuring bars whose lengths were known with an accuracy of ± 0.03 mm. Source and detector end corrections were known to within ± 0.25 mm.

III. SOURCES AND DETECTORS

The detection of photons and the techniques employed in maintaining acceptable spectral purity were different for the different photon sources. Each source-detector arrangement will be discussed separately below in the order of increasing photon energy. These discussions are summarized in Table I.

A. Vanadium 49

^{49}V decays 100% of the time by electron capture to the ground state of ^{49}Ti with a half-life of 330 days.[14] The weighted mean of the energies of the resulting Ti $K\alpha_1$ and $K\alpha_2$ x rays is 4.508 keV.[15] The difference between the $K\alpha_1$ and $K\alpha_2$ energies is negligible in a 1% measurement of an attenuation coefficient. Thus, in the experiments reported in this paper the $K\alpha$ lines are treated as a single line whose energy is the intensity weighted mean of the $K\alpha_1$ and $K\alpha_2$ energies. The weighted means of the $K\beta$ energies is 4.931 keV.[15] The Ti $K\alpha$-to-$K\beta$ intensity ratio[15] is 9.1. There is no element which has a K absorption edge between the Ti $K\alpha$ and $K\beta$ lines. Since the two sets of lines could not be resolved adequately with available detectors, it was necessary to employ an L edge filter to increase the $K\alpha$-to-$K\beta$ intensity ratio. Both the L_{II} and L_{III} edges of iodine fall between the Ti $K\alpha$ and $K\beta$ en-

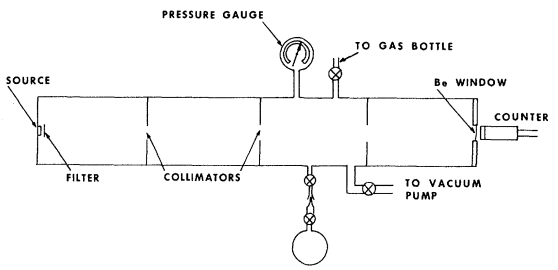

FIG. 1. Schematic diagram of typical experimental arrangement.

ergies. A $K\beta$ filter was fabricated by depositing about 2 mg/cm^2 of KI on a 0.001-in.-thick Be foil. The filtered $K\alpha$-to-$K\beta$ ratio of 30 was measured with a Si(Li) spectrometer and was checked periodically by measuring the transmissivity of the filter. There were no detectable iodine L radiations present. For all the gases except xenon the correction to μ/ρ due to the presence of the Ti $K\beta$ x rays was about 0.8%. Since the L_{III} edge of Xe falls between the $K\alpha$ and $K\beta$ lines of Ti, the effect of the Ti $K\beta$ radiation on the Xe measurements was critical. This effect was decreased by using Xe as an additional $K\beta$ filter for the Ti radiation and by calculating μ/ρ for Xe from count rates measured with two different pressures of Xe in the gas chamber. The resulting $K\alpha$-to-$K\beta$ ratio for the Xe measurement was 70 and the spectral impurity correction factor was 0.989.

The source consisted of 200 μCi of carrier-free solid ^{49}V mounted in a brass holder. The active material was covered with a layer of 0.0002-in.-thick Dupont "Kapton." Attenuation of the photons by this plastic film was negligible. The KI filter was mounted over the brass source holder. The diameter of the ^{49}V source was $\frac{1}{8}$ in.

The detector used in the ^{49}V experiments was a Harshaw Chemical Company "premium low-energy-type SHG" NaI (Tl) counter. The crystal was $\frac{1}{32}$ in. thick $\times \frac{31}{32}$ in. in diam. It was covered by a 0.005-in.-thick Be foil. The observed peak-to-valley ratio for the 4.508-keV x-ray photopeak was 15. A $\frac{3}{8}$-in.-diam Pb collimator was placed over the detector window. The diameter of the second collimator (which for this series of experiments was located one-third the distance from the source to the detector) was $\frac{1}{4}$ in. These collimators were cut from 0.017-in. Pb foil. Source-detector distances of 10–15 cm and gas pressures of 30–700 Torr were used.

B. Iron 55

^{55}Fe decays by electron capture to the ground state of ^{55}Mn with the emission of the characteristic Mn x rays. The half-life of ^{55}Fe is 2.6 years.[14] The weighted mean of the Mn $K\alpha_1$ and $K\alpha_2$ energies is 5.895 keV.[15] The $K\beta$ mean energy is 6.492 keV. The Mn $K\alpha$-to-$K\beta$ intensity ratio[15] is 8.4. Chromium is the only element whose K edge[15] (5.989 keV) lies between the $K\alpha$ and $K\beta$ energies of Mn. A Cr foil 0.0005 in. thick was used as a filter for the Mn $K\beta$ x rays. The filtered $K\alpha$-to-$K\beta$ ratio was ~400 as measured with a Si(Li) spectrometer. Weak Cr fluorescent x rays were observed. Their intensity was also lower than the Mn $K\alpha$ intensity by a factor of 400. No corrections to the measured attenuation coefficients were required by the presence of these spectral impurities.

The ^{55}Fe source strength was about 100 μCi. The material was obtained in the form of a liquid which was placed in a $\frac{1}{8}$-in.-diam $\times \frac{1}{32}$-in.-deep depression in a disk of tantalum metal. The liquid carrier (dilute HCl) was then evaporated, leaving the ^{55}Fe deposited in the source holder. The Cr filter was mounted on the holder over the $\frac{1}{8}$-in.-diam source.

The detector, geometry, and gas pressures for the ^{55}Fe experiments were the same as those used in the ^{49}V experiments described previously. Longer gas lengths (10–50 cm) were used.

C. Germanium 71

^{71}Ge decays by electron capture to the ground state of ^{71}Ga with the emission of the characteristic Ga x rays. The half-life of ^{71}Ge is 11.4 days.[14] This is the shortest half-life of any of the sources used in these experiments. Because of the source strength and the data-taking sequence (to be discussed later) no corrections to the data due to the short half-life were required. The weighted mean of the Ga $K\alpha_1$ and $K\alpha_2$ energies is 9.243 keV.[15] The weighted mean of the $K\beta$ energies is 10.263 keV. The K absorption edge of zinc (9.659 keV) is between the $K\alpha$ and $K\beta$ energies of Ga. A Zn foil whose thickness was 0.0015 in. was used as a filter for the Ga $K\beta$ x rays. The $K\alpha$-to-$K\beta$ intensity ratio of the filtered source was ~300 as measured with a Si(Li) spectrometer. Fluorescent x rays from the Zn filter were detected. Their intensity was about $\frac{1}{200}$ times that of the Ga $K\alpha$ x ray. No corrections to the measured attenuation coefficients were required due to spectral impurities.

The ^{71}Ge source strength was 15 mCi upon receipt from the isotope vendor. The high specific activity solid material was mounted in a brass source holder which was covered with the 0.0015-in.-thick Zn $K\beta$ filter. The diameter of the ^{71}Ge source was $\frac{1}{8}$ in.

The detector for the ^{71}Ge experiments was the same as that used in the ^{49}V and ^{55}Fe experiments. The experimental geometry was slightly different in that longer source-detector distances (10–90 cm) and higher gas pressures (100–1800 Torr) were used.

D. Iodine 125

^{125}I decays by electron capture to the first excited state (35.48 keV) of ^{125}Te with the emission of the characteristic Te x rays. The Te decays by γ-ray emission 7% of the time. The half-life of ^{125}I is 60 days.[14] The weighted mean of the Te $K\alpha_1$ and $K\alpha_2$ energies is 27.380 keV.[15] The weighted mean of the $K\beta$ energies is 31.128 keV. These three photon lines (x rays and γ ray) were well resolved with a Ge(Li) spectrometer. The count rate in the pulse-height spectrum dropped to background be-

tween the photopeaks. This detector was used in making the attenuation-coefficient measurements with the ^{125}I source. A single-channel analyzer was adjusted tightly on the Te $K\alpha$ photopeak. The count rates thus measured contained negligible contributions from the two higher-energy peaks due to the detector resolution, and to the lack of Compton scattering in Ge at 35 keV.

The carrier-free solid ^{125}I source had a strength of 30 mCi. It was mounted in a brass source holder which was sealed with a thin plastic window. The diameter of the ^{125}I source was $\frac{1}{8}$ in.

The experimental geometry used with this source involved source-detector distances 122–183 cm. The 1-cm-diam detector was mounted outside the gas chamber which it viewed through a 0.010-in.-thick Be foil. One $\frac{1}{4}$-in.-diam collimator was used with all source-detector distances. A $\frac{3}{8}$-in. Pb collimator was mounted over the detector. Gas pressures of 108–2600 Torr were used in this series of measurements.

E. Dysprosium 159

^{159}Dy decays by electron capture to ^{159}Tb. 74% of the decays go directly to the ground state, 26% to the first excited state at 58 keV, and a negligible fraction to higher states in ^{159}Tb. 4% of the ^{159}Dy disintegrations result in 58-keV ^{159}Tb γ rays. The half-life of ^{159}Dy is 144 days.[14] The weighted mean of the Tb $K\alpha_1$ and $K\alpha_2$ x-ray energies is 44.229 keV.[15] The mean $K\beta$ energy is 50.650 keV. The x rays and γ ray were well resolved with a Ge(Li) spectrometer; the count rate in the pulse-height spectrum dropped to background between the photopeaks. The Ge(Li) detector was used in measuring the gas attenuation coefficients with the ^{159}Dy source. A single-channel analyzer was adjusted on the Tb $K\alpha$ photopeak. The count rates thus measured contained negligible contributions from the two higher-energy peaks due to the detector resolution and to the lack of Compton scattering in Ge at 58 keV.

The high-specific-activity solid ^{159}Dy source had a strength of 30 mCi. It was mounted in a brass source holder which was sealed with a thin plastic window. The source diameter was $\frac{1}{8}$ in.

The experimental geometry used with ^{159}Dy involved source-detector distances ranging from 91 to 366 cm. The 1-cm-diam detector was mounted outside the gas chamber which it viewed through a 0.010-in.-thick Be foil. One or two collimators $\frac{3}{8}$ in. in diam were used to prevent the scattering of photons into the detector by the gas and by the walls of the chamber. Gas pressures of 75–3100 Torr were used in these measurements.

F. Cadmium 109

^{109}Cd decays by electron capture to the 40-sec isomeric first excited state of ^{109}Ag.[14] This state deexcites 5% of the time by γ-ray emission. The energy of this γ ray has recently been determined to be 88.09 keV,[16] slightly above the Pb K edge.[17] The half-life of ^{109}Cd is 453 days.[14] A NaI counter was used in the ^{109}Cd experiments. It contained a $1\frac{1}{4}$-in.-diam$\times\frac{1}{4}$-in.-thick NaI(Tl) crystal mounted on a 2-in.-diam photomultiplier tube. The resolution of the counter was 14% full width at half-maximum (FWHM) at 88 keV. A single-channel analyzer was adjusted on the photopeak of the 88-keV γ ray.

The Ag x rays emitted by the ^{109}Cd source were 20 times more intense than the γ rays which were used in the attenuation-coefficient measurements. For the shorter sample lengths (< 400 cm) used with Ar, Kr, and Xe, the count rates were sufficiently high so that the pile-up of Ag x rays in the NaI counter was non-negligible. In order to eliminate this problem, a molybdenum filter whose thickness was 0.015 in. was placed over the ^{109}Cd source. This filter removed essentially all the Ag x rays while passing over half of the γ rays.

TABLE I. Summary of source-dectector parameters.

Energy (keV)	Source and source strength (mCi)	Half-life	Detector	Method of discriminating against spectral impurities
4.508	^{49}V – 0.2	330 days	NaI	KI $K\beta$ filter
5.895	^{55}Fe – 0.1	2.6 yr	NaI	Cr $K\beta$ filter
9.243	^{71}Ge – 15	11.4 days	NaI	Zn $K\beta$ filter
27.380	^{125}I – 30	60 days	Ge(Li)	single-channel analyzer adjusted on resolved $K\alpha$ photopeak
44.229	^{159}Dy – 30	144 days	Ge(Li)	single-channel analyzer adjusted on resolved $K\alpha$ photopeak
88.09	^{109}Cd – 100	453 days	NaI	Mo filter for Ag x rays
145.43	^{141}Ce – 30	33 days	NaI	Mo filter for β particles and Pr x rays

For the longer sample length (733 cm) used in the air and neon measurements, a 0.005-in.-thick Mo filter was used.

The ^{109}Cd source contained 100 mCi of high-specific-activity solid material mounted in a brass source holder. The source diameter was $\frac{1}{4}$ in. It was covered with a thin plastic film.

The ^{109}Cd experiments utilized source-detector distances of 60–733 cm. The detector end of the gas chamber contained a $\frac{1}{16}$-in.-thick Al window over which was mounted a $1\frac{1}{4}$-in.-diam collimator made of $\frac{1}{8}$-in.-thick Pb for the longer sample lengths. For the shorter distances, a $\frac{1}{2}$-in.-diam detector collimator was used. One to three other collimators were placed at equal intervals along the length of the chamber. Their aperture diameters were slightly larger than the cone subtended by the detector at the source. Gas pressures ranged from 800–3600 Torr.

G. Cerium 141

^{141}Ce β decays to ^{141}Pr with a half-life of 33 days.[14] 70% of the β's go to the first excited state in ^{141}Pr at[14] 145.43 keV and 30% go to the ground state. 48% of the ^{141}Ce β decays[14] lead to the production of 145.43-keV ^{141}Pr γ rays. These γ rays were used in the present gas attenuation-coefficient measurements. To prevent possible difficulties caused by Pr x rays and β particles (0.581-MeV end-point energy) a 0.005-in.-thick molybdenum filter was placed over the ^{141}Ce source. This filter absorbed all of the β's, most of the x rays, and 5% of the γ rays. The photon spectrum emitted by the ^{141}Ce source was studied with a Ge(Li) spectrometer. The ^{139}Ce γ ray at 166 keV was detectable with an intensity of $<1\%$ that of the 145-keV γ ray. A single-channel analyzer, set tightly on the 145-keV photopeak, prevented these higher-energy γ rays from contributing to the present measurements.

The detector, experimental geometry, and gas pressures were the same as those used in the ^{109}Cd experiments discussed above. The ^{141}Ce source contained 30 mCi of high-specific-activity solid material mounted in a brass holder. The source diameter was $\frac{1}{8}$ in. It was sealed with a 0.001-in.-thick brass foil.

IV. SAMPLES

Samples of "research grade" noble gases were purchased commercially. Quantitative analyses performed by the vendor indicated that the gases had the following purities: neon, 99.99%; argon, 99.999%; krypton, 99.995%; and xenon, 99.995%. Mass-spectrometric analyses of samples of the gases taken during these experiments revealed that most of the gases contained less than 100 ppm of impurities. The only exception was krypton which contained 0.01–0.03% of xenon. A few of the samples contained detectable quantities of air. None of the noble gases contained sufficient impurities to necessitate corrections to the measured attenuation coefficients.

The measurement of the air attenuation coefficient at 4.508 keV made use of atmospheric air. As duscussed in Ref. 10, no impurity corrections were required in this measurement. The higher-energy air measurements required pressures greater than 1 atm. Pressurized bottles of air were acquired from a local diver's supply vendor. Air processed for this purpose is filtered in order to remove moisture and oil vapors. Mass-spectrometric analyses of air samples taken from the diver's bottles revealed that the relative quantities of the major constituents of the compressed air were the same as those of atmospheric air. There were no detectable impurities present in the bottles of compressed air. As a final check on the air purity, the experiment reported in Ref. 10 was repeated using compressed air. The measured attenuation coefficient of air at 5.895 keV using the compressed air was 24.50 cm^2/g compared with 24.55 ± 0.25 cm^2/g reported in Ref. 10, well within quoted experimental errors. The errors introduced into the present measurements due to the composition and purity of the compressed air were negligible.

In order to calculate the mass attenuation coefficient from the measured count rates, the gas sample thickness in g/cm^2 is required. This thickness is the product of the sample length and density. The gas density was obtained by applying pressure and temperature corrections to handbook[18] values of the STP densities. These corrections were applied assuming the validity of the perfect gas law as follows:

$$\rho = \rho_0 (P/P_0) 273.15/(273.15 + T) , \qquad (2)$$

where ρ is the density of the gas at the pressure P and temperature T (°C). P_0 is atmospheric pressure (760 Torr), and ρ_0 is the density of the gas at standard temperature and pressure. The values of ρ_0 used in analyzing the data were 0.89990×10^{-3} g/cm^3 for neon, 1.7837×10^{-3} g/cm^3 for argon, 3.733×10^{-3} g/cm^3 for krypton, 5.887×10^{-3} g/cm^3 for xenon, and 1.2929×10^{-3} g/cm^3 for air. For the pressures and temperatures used in these experiments, the error introduced by assuming the validity of the perfect-gas law was negligible.

V. EXPERIMENTAL PROCEDURE

In addition to the sample thickness, other quantities required for the calculation of μ/ρ are the unattenuated photon beam intensity, the attenuated photon beam intensity, and the background count rate. Unattenuated count rates varied from 30

(^{49}V source at 15 cm) to 5000 counts/sec (^{71}Ge source at 10 cm). Dead time in the NaI counter was shown to be negligible for these count rates. Except for the Xe measurement at 4.5 keV all unattenuated count rates were measured with the gas-chamber pressure below 5×10^{-3} Torr. Background count rates were measured by placing a Pb plate over the source. For most of the experiments, the background count rate was much less than 1% of the unattenuated count rate. The only exceptions were the air, neon, and argon measurements made with the ^{141}Ce source, where the background count rates were between 1% and 3% of the unattenuated count rates.

Counting times, depending upon the count rate, varied from 100 to 2000 sec. For each data point, counts were taken in the following sequence: background, five vacuum counts, background, five sample counts, background, five sample counts, background, five vacuum counts, background. All of the counting times were the same during a given sequence. During each sample count the sample pressure and temperature were measured. Sufficient counts were taken during most of the experiments so that the value of μ/ρ calculated from each individual sample count contained a statistical error of 1% or less. The above data taking sequence was carried out from three to five times for each gas-energy experiment. Between these sequences the sample length and/or sample pressure were changed. Whenever possible, transmissivities of 0.5 or less were used. Constraints imposed by maximum sample length and pressure, however, made this impossible for some of the experiments.

VI. DATA ANALYSIS

From the data taken in the above-mentioned sequence, the measured values of μ/ρ were calculated as follows:

$$\frac{\mu}{\rho} = -\frac{\ln(I/I_0)}{\rho l} \quad , \tag{3}$$

where μ/ρ is the mass attenuation coefficient in cm^2/g, I is the attenuated count rate, I_0 is the unattenuated count rate, ρ is the sample density in g/cm^3, and l is the sample length in cm. I_0 is the mean of five vacuum counts from which was subtracted the mean of the background counts taken before and after the vacuum counts. I is a single sample count from which was subtracted the mean of the background counts taken before and after the set of five sample counts containing I. ρ was calculated from Eq. (2) using the values of P and T measured during the sample count I. The value of I_0 used in Eq. (3) was the one measured nearest in time to the value of I being used. Thus in the data-taking sequence the first measure of I_0 was used with the first five values of I, etc.

A single sequence of counts resulted in ten measurements of μ/ρ. Because of the data-taking sequence, errors due to source decay tend to cancel. The only source whose decay rate could have introduced error was ^{71}Ge. This source was sufficiently strong so that a single data sequence required less than an hour, during which time the error in μ/ρ due to the linear approximation to the source decay rate was negligible.

The only deviation in the data-taking and data-analysis procedures occurred in the xenon experiment at 4.5 keV. In this instance Xe gas was used as an additional $K\beta$ filter. The unattenuated count rate I_0 was measured with a pressure of 35 Torr of Xe in the gas chamber. The Xe pressure was increased before the attenuated count rate was measured. The value of ρ used in Eq. (3) was calculated from Eq. (2), where P was the increase in pressure between the two count-rate measurements.

The results obtained at 4.508 keV were the only ones to which corrections due to spectral impurities were applied. For the air, Ne, Ar, and Kr experiments, the measured $K\alpha/K\beta$ intensity ratio of the filtered ^{49}V source was 30. For the Xe measurement, the ratio was 70. Using the compiled attenuation coefficients from Ref. 15, factors were calculated by which the measured coefficients were multiplied to correct for the presence of the $K\beta$ radiation. This factor was 1.0081 for air, 1.0078 for Ne, 1.0085 for Ar, 1.0077 for Kr, and 0.989 for Xe. The corrections are small and are not sensitive to an accurate determination of the $K\alpha/K\beta$ intensity ratio.

No corrections were made to any of the results due to the presence of sample impurities. In every case such corrections would have amounted to less than 0.1% of the measured values of μ/ρ.

VII. THEORETICAL CALCULATIONS

The total photon cross sections of air, Ne, Ar, Kr, and Xe were calculated at the energies for which the measurements were made. The composition of air was assumed to be 75.5-wt.% N_2, 23.2-wt.% O_2, and 1.3-wt.% Ar. In this energy region, the total cross section, $(\mu/\rho)_t$ in cm^2/g, is given by

$$(\mu/\rho)_t = (\mu/\rho)_\tau + (\mu/\rho)_i + (\mu/\rho)_c \quad , \tag{4}$$

where $(\mu/\rho)_\tau$ is the photoelectric cross section, $(\mu/\rho)_i$ is the total incoherent cross section for a bound electron, and $(\mu/\rho)_c$ is the coherent scattering cross section. Each of these cross sections was calculated separately, using what are considered to be the best experimental and theoretical data and calculational methods currently available.

The photoelectric cross sections were computed by a modified version of the Brysk-Zerby method,[19] which uses bound-state wave functions and potentials from a relativistic Dirac-Slater self-consistent-

TABLE II. Measured attenuation coefficients in cm^2/g.

Energy (keV)	Air	Ne	Ar	Kr	Xe
4.508	54.0 ±0.9	125 ±2	558 ±8	466 ±8	278 ±5
5.895	24.55 ±0.25[a]	57.0 ±0.7	274 ±3	227 ±3	672 ±8
9.243	6.34 ±0.08	15.0 ±0.2	79.7 ±1.0	66.0 ±0.8	210 ±3
27.380	0.406±0.005	0.713±0.008	3.46 ±0.04	23.9 ±0.3	11.25 ±0.13
44.229	0.227±0.003	0.296±0.003	0.936±0.012	6.26 ±0.07	17.2 ±0.2
88.09	0.160±0.002	0.169±0.002	0.237±0.003	0.992±0.012	2.79 ±0.03
145.43	0.137±0.002	0.138±0.002	0.146±0.002	0.315±0.004	0.763±0.010

[a]See Ref. 10.

field program.[20] The wave functions used in the present calculations differ slightly from those described in Ref. 20 because of an improved treatment of the Slater exchange term.[21] A further modification of the Brysk-Zerby method includes the use of experimentally determined values of electron binding energies[22] in these calculations, rather than computed energy eigenvalues. The derivation of the photoelectric cross section is given by Rakavy and Ron,[23] and details of the numerical methods used are given in a technical report.[24] In the present calculations, the photoelectric cross section of each electron subshell was computed and the contributions of all subshells were summed to give the total cross section at each energy.

The total incoherent cross section for bound electrons, $(\mu/\rho)_i$, was calculated from

$$\frac{d(\mu/\rho)_i}{d\Omega} = \frac{d(\mu/\rho)_{KN}}{d\Omega} S(q, Z)$$

$$= \frac{r_0^2 Z}{2} \frac{1}{[1+\alpha(1-\cos\theta)]^2}$$

$$\left(1+\cos^2\theta + \frac{\alpha^2(1-\cos\theta)^2}{1+\alpha(1-\cos\theta)}\right) S(q, Z) \quad (5)$$

by numerical integration over the scattering angle θ. In (5), $\alpha = h\nu_0/m_0c^2$ and r_0 is the classical electron radius. $d(\mu/\rho)_{KN}/d\Omega$ is the differential form of the Klein-Nishina equation, which gives the probability that the photon is deflected at a given angle and transfers momentum to the electron as if it were free. $S(q, Z)$ is the incoherent scattering function which gives the probability that an atom will be raised to an ionized or excited state when the photon imparts recoil momentum $\vec{q}$ to an atomic electron. The incoherent scattering functions used for the spherically symmetric free atoms are those calculated by Cromer and Mann,[25] which were computed with Hartree-Fock wave functions using all exchange terms. For the aspherical free atoms, the incoherent scattering factors calculated by Cromer[26] were used. These scattering factors were also computed with Hartree-Fock wave functions using all exchange terms.

The coherent-scattering cross section $(\mu/\rho)_c$ was calculated from

$$\frac{d(\mu/\rho)_c}{d\Omega} = \tfrac{1}{2} r_0^2 (1+\cos^2\theta) F^2(q, Z) \quad (6)$$

by numerical integration over the scattering angle θ. In (6), r_0 is the classical electron radius, and $F(q, Z)$ is the form factor which gives the probability that the recoil momentum $\vec{q}$ is transferred to the Z electrons with no energy absorption. The form factors used in these calculations were computed by Cromer.[27]

VIII. RESULTS

The results of the experimental measurements are listed in Table II. The quoted errors include random errors due to counting statistics and estimates of other possible random and systematic errors. Each coefficient is the mean of from 30 to 50 individual measurements. Most of the coefficients were measured at more than one sample pressure and length. There were no differences in the values of the measured coefficients which could be attributed to these changes in geometry and sample thickness.

The results of the theoretical calculations are presented in Table III. The agreement between the experimental results and the theoretical predictions is considered to be good.

IX. ERRORS

Possible sources of error in the experimental measurements include the following: (a) counting

TABLE III. Calculated attenuation coefficients in cm^2/g.

Energy (keV)	Air	Ne	Ar	Kr	Xe
4.508	52.74	122.7	555.5	445.0	272.5
5.895	23.80	55.93	271.3	216.9	663.3
9.243	6.253	14.72	78.09	63.98	206.6
27.380	0.4056	0.7155	3.454	23.75	11.27
44.229	0.2269	0.2988	0.9408	6.331	17.50
88.09	0.1607	0.1694	0.2388	0.9822	2.793
145.43	0.1368	0.1383	0.1452	0.3142	0.7655

statistics, (b) beam-intensity measurements, (c) pressure, temperature, and length measurements, (d) gas purity, (e) photon beam spectral purity, and (f) finite geometry. These errors and estimates of their magnitude will be discussed separately.

a. Counting statistics. Sufficient counts were taken in all of the experiments to assure that the random error due to counting statistics was less than 0.5%. Each coefficient is the mean of 30 to 50 individual measurements. The standard deviation for a single measurement was approximately 1% for most of the experiments. In the air and neon experiments at 88 and 145 keV, the transmissivities were high and the standard deviation for a single measurement ran as high as 1.5%. For all of the experiments, however, the standard deviation of the mean ($\sigma/N^{1/2}$) was less than 0.5%.

b. Beam-intensity measurements. Systematic errors in count-rate measurements cancel since count rates enter only as a ratio [Eq. (2)]. Errors in μ/ρ due to source decay and electronic variations are negligible (<0.1%) due primarily to the data-taking sequence used in the measurements.

c. Pressure, temperature, and length measurements. For most of the measurements, errors in μ/ρ due to errors in P-T-L measurements, were negligible. For experiments involving low pressure and short sample lengths, systematic errors in μ/ρ could have been as high as 1%, due to combined pressures and length measurements. Error in μ/ρ due to temperature measurement was negligible.

d. Gas purity. Errors in μ/ρ due to sample impurities were less than 0.1% for all of the measurements.

e. Photon beam spectral purity. The only photon source whose spectrum contained appreciable impurities was the ^{49}V source. A small correction was applied to the measured coefficients to remove the effect of the Ti $K\beta$ x rays. The effect of spectral impurities on the measured attenuation coefficients was less than ±0.2%.

f. Finite geometry. Small-angle scattering of photons into the detector, and miltiple Compton scattering by the chamber walls, collimators, and gas would tend to lower the measured attenuation coefficients. For the higher-energy measurements, where this effect could be non-negligible, the beam geometry was much tighter and the number of collimators was larger. Because of the narrow-beam geometry used in these experiments, errors in the measured values of μ/ρ due to finite geometry were <0.05% and were neglected.

An estimate of the combined errors is listed in Table II with the measured coefficients. They vary from 1% for most of the measurements to nearly 2% for the low-energy high-Z experiments.

The accuracy of the calculational methods was investigated by comparing computed total cross sections with an extensive set of measured cross sections.[17,28] The comparison was made for 24 elements with atomic numbers ranging from 4 through 94 over the energy region of 25 keV to 1.6 MeV. The calculated cross sections typically agree to better than 2% with the experimental values. Based on this comparison, the accuracy of the calculated cross sections reported here is estimated to be ±2%.

ACKNOWLEDGMENTS

The authors gratefully acknowledge the gas analyses performed by Dr. R. M. Alire and Dr. E. D. Loughran of the Los Alamos Scientific Laboratory.

*Work performed under the auspices of the U.S. Atomic Energy Commission.

†EG&G summer student from California Institute of Technology, Pasadena, Calif.

[1]B. L. Henke, *Advances in X-Ray Analysis* (Plenum, New York, 1970), Vol. 13.

[2]Alan J. Bearden, J. Appl. Phys. 37, 1681 (1966).

[3]F. Wuilleumier, J. Phys. (Paris) 26, 776 (1965).

[4]A. P. Lukirskii and T. M. Zimkina, Izv. Akad. Nauk SSSR 27, 817 (1963) [Bull. Acad. Sci USSR 27, 333 (1963)].

[5]J. A. Crowther and L. H. H. Orton, Phil. Mag. 10, 329 (1930); 13, 505 (1932).

[6]R. G. Spencer, Phys. Rev. 38, 1932 (1931).

[7]B. Woernle, Ann. Physik 5, 475 (1930).

[8]W. W. Colvert, Phys. Rev. 36, 1619 (1930).

[9]S. J. M. Allen, reported in A. H. Compton and S. K. Allison, *X-Rays in Theory and Experiment* (Van Nostrand, New York, 1935).

[10]J. H. McCrary, L. H. Ziegler, and L. D. Looney, J. Appl. Phys. 40, 2690 (1969).

[11]A. P. Lukirskii, I. A. Brytov, and T. M. Zimkina, Opt. Spektroskopiya 17, 438 (1964) [Opt. Spectry. (USSR) 17, 234 (1964)].

[12]F. Wuilleumier, thesis, University of Paris, 1969 (unpublished).

[13]A. R. P. Rau and U. Fano, Phys. Rev. 167, 7 (1968).

[14]C. M. Lederer, J. M. Hollander, and I. Perlman, *Table of Isotopes*, 6th ed. (Wiley, New York, 1967).

[15]E. Storm and H. I. Israel, LASL Report No. LA-3753, 1967 (unpublished).

[16]C. Foin, A. Gizon, and J. Oms, Nucl. Phys. A113, 241 (1968).

[17]A. L. Conner, H. F. Atwater, Elizabeth H. Plassmann, and J. H. McCrary, Phys. Rev. A 1, 539 (1970).

[18]*Handbook of Chemistry and Physics*, 48th ed., edited by R. C. Weast (The Chemical Rubber Co., Cleveland, Ohio, 1967).

[19]H. Brysk and C. D. Zerby, Phys. Rev. 171, 292 (1968).

[20]D. Liberman, J. T. Waber, and Don T. Cromer, Phys. Rev. 137, A27 (1965).

[21]Don T. Cromer (private communication).

[22]J. A. Bearden, Report No. NSRDS-NBS 14, 1967 (unpublished).

[23]G. Rakavy and A. Ron, Phys. Rev. 159, 50 (1967).
[24]H. Brysk and C. D. Zerby, Union Carbide Corporation Report No. UCC/DSSD-229, 1967 (unpublished).
[25]Don T. Cromer and Joseph B. Mann, J. Chem. Phys. 47, 1892 (1967).
[26]Don T. Cromer, J. Chem. Phys. 50, 4857 (1969).
[27]Don T. Cromer, (unpublished).
[28]J. H. McCrary, Elizabeth H. Plassmann, J. M. Puckett, A. L. Conner, and G. W. Zimmermann, Phys. Rev. 153, 307 (1967).

PHYSICAL REVIEW A VOLUME 2, NUMBER 6 DECEMBER 1970

Molecular Description of Nematic Liquid Crystals

T. C. Lubensky*†
Laboratoire de Physique des Solides,† Faculté des Sciences, 91-ORSAY, France
(Received 8 June 1970)

Liquid crystals are considered as gases of long barlike molecules. Variables describing the position and orientation of individual molecules are introduced. These are used to arrive at a microscopic definition of the order in liquid crystals in terms of a symmetric traceless tensor. The Frank and Leslie-Ericksen directors are shown to be equivalent to the unit eigenvector associated with the largest eigenvalue of this symmetric traceless tensor. Attention is then restricted to nematics. It is shown that the Frank free energy gives a valid description of equilibrium properties of nematics to order $\chi^a H^2/\rho k T m^{-1}$, where χ^a is the anisotropic magnetic susceptibility, H the external magnetic field, ρ the mass density, T the temperature, k the Boltzmann constant, and m the molecular mass. Microscopic justification is given for the linearized Leslie-Ericksen hydrodynamic theory for nematics. A microscopic response-function description of nematics is then presented, and contact is made between the general frequency- and wave-number-dependent response functions and those calculated from the phenomenological hydrodynamic theory. Applications to light scattering and nuclear magnetic resonance are considered. $1/T_1$ calculated here differs from that calculated from the Pincus theory by a factor of S^2, where S is the parameter measuring the degree of nematic order.

I. INTRODUCTION

The liquid-crystalline state of matter is a state intermediate between a solid crystal and a liquid.[1,2] This state of matter has been the subject of much research since its discovery by the Austrian botanist Reinitzer at the end of the last century.[3] Early experiments showed that certain organic crystals when melted produced a liquid of turbid appearance which upon further heating underwent another transition to an isotropic transparent liquid. This turbid-appearing state was soon shown to have anisotropic optical, electrical, and magnetic properties and was named the liquid-crystalline state by Lehman.[4] This state, though anisotropic, still flowed like a liquid. Furthermore, x-ray experiments indicated a random arrangement of the centers of mass of the molecules in the liquid.[1,2] Later, experiments were able to link the observed anisotropies with alignment along a certain direction of the long molecules which compose the liquid crystal. In 1922 Friedel[5] distinguished the following subclasses of the liquid-crystalline state according to the properties of single-crystal samples:

Nematic state. The centers of mass of the elongated molecules are randomly oriented but their long axes are oriented along a specific direction. There is rotational invariance about the direction of alignment [Fig. 1(a)].

Smectic state. The centers of mass of the molecules are arranged in parallel equidistant planes. Motion of the centers of mass in each plane is allowed. The long axes of the molecules are aligned along a specific direction [Fig. 1(b)].

Cholesteric state. A subclass of the nematic state in which the direction of orientation rotates in a screwlike motion [Fig. 1(c)].

In order to describe deformations in liquid crystals, Frank[6] and later Ericksen[7] following an idea of Oseen[8] introduced at each point in space a phenomenological unit vector $n_i(\vec{r})$ describing the orientation of the molecules at that point. Frank then discussed the possible functional dependence of the free energy on $n_i(\vec{r})$ and its first spatial derivative subject to the condition that $n_i(\vec{r})$ and $-n_i(\vec{r})$ be equivalent configurations. He found that the free energy in a nematic could be expressed as

$$F = \tfrac{1}{2}\int d^3r \{K_{11}(\vec{\nabla}\cdot\vec{n})^2 + K_{22}[\vec{n}\cdot(\vec{\nabla}\times\vec{n})]^2 + K_{33}[\vec{n}\times(\vec{\nabla}\times\vec{n})]^2 - (K_{22}+K_{24})[(\vec{\nabla}\cdot\vec{n})^2 - \nabla_i n_j \nabla_j n_i]\}, \quad (1.1)$$

where K_{11}, K_{22}, K_{33}, and K_{24} are elastic constants. The first term in this equation, in the language of Frank, gives the energy associated with splay [Fig. 2(a)], the second that associated with torsion, and the third that associated with flexion [Fig. 2(c)].